J. Fluid Mech. (1968), *vol.* 31, *part* 2, *pp.* 321–342
Printed in Great Britain

Magnetohydrodynamic flow along cylindrical pipes under non-uniform transverse magnetic fields

By L. TODD

Department of Mathematics, University of Strathclyde, Glasgow, C. 1

(Received 11 July 1967)

The unidirectional flow of an incompressible, electrically conducting, viscous fluid along cylindrical pipes is considered. An external magnetic field, $\mathbf{B}_0$, which lies in the plane transverse to the flow is applied. It is shown that the governing equations, written in the co-ordinate system traced out by $\mathbf{B}_0$, are mathematically very similar to those for a uniform field.

The paper deals mainly with ducts whose walls are insulators. Though exact solutions (valid for all values of the Hartmann number) are derived, the limit of high Hartmann number is taken for detailed discussion. Transition layers (or, loosely, 'wakes') can arise which are centred on *curved* field lines. In some cases, reversed flow occurs in part of the core ('radial-type' fields). Situations also arise where the magnitude (and sign) of the velocity remains the same as for $\mathbf{B}_0 = 0$, whatever the strength of the applied, transverse (azimuthal) magnetic field.

1. Introduction

Problems associated with pressure driven flows of electrically conducting fluid have attracted considerable attention. Almost always the applied, transverse magnetic field lines are parallel. A few workers, e.g. Globe (1959), have considered a radial field. In this paper, a proper examination of the general case is given. It is fairly well known that the governing equations are linear whatever the form of $\mathbf{B}_0$, the applied transverse magnetic field. If the orthogonal, curvilinear co-ordinate system appropriate to $\mathbf{B}_0$ is used, the governing equations are very similar to those for uniform fields. In fact, each exact solution derived for a specific $\mathbf{B}_0$ can be generalized to cover any transverse field.

For a duct of arbitrary cross-section with insulating walls, the main features of the flow in the limit of large Hartmann number are derived by boundary-layer techniques (see §3). For a rectangular† duct, the exact solution is also given. The above pair of results are applied to two explicit cases. In the first, the field lines are curved; $\mathbf{B}_0$ varies between field lines but not along them. In the second, the field lines are radial; $\mathbf{B}_0$ varies along the field lines but not normal to them. The exact solution is given for flow through an annular channel, when the field lines are closed loops and each boundary coincides with a field line. A boundary-layer approach is also employed, in the limit of large Hartmann number. The

† One pair of sides are aligned with $\mathbf{B}_0$, the other pair are normal to the applied field.

latter type of analysis is carried out for the case where the field is normal to the walls of the annulus.

Many novel features arise, due to the non-uniformity of $\mathbf{B}_0$. These are fully discussed as, and where, they arise. M.K.S. units are employed throughout this paper and as far as possible, the notation is standard.

2. The governing equations

Steady, laminar, unidirectional flow along a cylindrical pipe is to be examined. In addition, it is required that pressure varies linearly with distance, z, along the pipe and that no other quantity varies with z. At this stage, the discussion is limited to finding out if such a flow is consistent with the equations governing magneto-hydrodynamic flows. Since there is no time dependence, the electric field satisfies

$$\operatorname{curl} \mathbf{E} = 0. \tag{1}$$

Also, there is only variation with x and y, and so equation (1) requires that

$$\partial E_z/\partial y = \partial E_z/\partial x = 0.$$

This means that E_z is constant. In fact, the value of E_z is something that can be set by the design of the experiment. This paper is devoted to the case

$$E_z = 0, \tag{2}$$

i.e. there is no potential difference between the ends of the channel. Since the flow is in the z-direction it follows from

$$\mathbf{j} = \sigma(\mathbf{E} + \mathbf{V} \wedge \mathbf{B}) \tag{3}$$

that current lines lie in the (x, y)-plane. Here $\mathbf{j}$ represents current, $\mathbf{v}$ velocity, $\mathbf{B}$ magnetic field and σ electrical conductivity. Let

$$\mathbf{B} = \mathbf{B}_0 + (\mathbf{B}.\hat{\mathbf{z}})\hat{\mathbf{z}}.$$

Now, $\operatorname{div} \mathbf{B} = 0$ and B_z depends only on x and y. Thus

$$\operatorname{div} \mathbf{B}_0 = 0. \tag{4}$$

As $\mu\mathbf{j} = \operatorname{curl} \mathbf{B}$, it can be deduced from equation (3) that

$$\operatorname{curl} \mathbf{B}_0 = 0. \tag{5}$$

The flow which is being examined is the large time limit of an unsteady flow. Two ways in which the flow can be set up are immediately apparent. The magnetic field could be gradually switched on; the flow being initially the appropriate Poiseuille one. Alternatively, the pressure difference between the ends of the channel could be gradually increased from zero to the desired value. In each of the above cases, a precursory examination shows that B_z remains zero outside the current loops and that the applied transverse field remains unaffected† by the flow. Consequently, $\mathbf{B}_0$ is the *applied* transverse magnetic field. Equations (4) and (5) are consistent with the latter fact.

The governing equations are (cf. Shercliff 1953)

$$\rho\nu\nabla^2 V_z + (\mathbf{B}_0.\nabla)(B_z/\mu) = -P, \tag{6}$$

$$\lambda\nabla^2 B_z + (\mathbf{B}_0.\nabla) V_z = 0, \tag{7}$$

$$\partial/\partial x, \partial/\partial y\,(p + (B_z^2/2\mu)) = 0, \tag{8}$$

† It is assumed that $\mathbf{V} = V_z\hat{\mathbf{z}}$ and $\partial/\partial z \equiv 0$, with the one exception that $\partial p/\partial z = -P(t)$.

$-P = \partial p/\partial z =$ constant. The positive z-direction is chosen to be that which gives $P > 0$. Equation (8) indicates the absence of forces tending to swirl the fluid or move it across the pipe. B_z is the stream function for current, i.e. current flows along the lines $B_z =$ constant. In equations (6)–(8), ρ represents density, ν kinematic viscosity and μ permeability.

$\mathbf{B}_0$ is a two-dimensional vector function. By virtue of equations (4) and (5) we can define a potential $\phi(x, y)$, and a stream function $\psi(x, y)$, such that

$$\mathbf{B}_0 = B^* L \nabla\phi = B^* L \operatorname{curl}(\psi\hat{\mathbf{z}}). \tag{9}$$

L is a reference length. B^* is a reference value for the applied field. These two quantities will be explicitly defined very shortly. The curves $\phi =$ constant and $\psi =$ constant form an orthogonal, curvilinear co-ordinate system. The problem is better suited to this 'natural' co-ordinate frame. The scale factor for the ϕ co-ordinate is h_ϕ and that for the ψ co-ordinate, h_ψ. The transformation between the non-dimensional variables $\{(x/L), (y/L)\}$ and $\{\phi, \psi\}$ corresponds to a conformal mapping. The equati ons (9) become

$$B_0\hat{\boldsymbol{\phi}} = (B^*/h_\phi)\,\hat{\boldsymbol{\phi}} = (B^*/h_\psi)\,\hat{\boldsymbol{\phi}}.$$

Thus
$$h_\phi = h_\psi = \{B^*/B_0(\phi, \psi)\} = (M^*/M), \tag{10}$$

where
$$M = \{\sigma^{\frac{1}{2}} B_0 L/(\rho\nu)^{\frac{1}{2}}\} \quad \text{and} \quad M^* = (\sigma^{\frac{1}{2}} B^* L/(\rho\nu)^{\frac{1}{2}}). \tag{11}$$

M is the 'local' value of the Hartmann number. In later sections, the 'Hartmann vector', $\boldsymbol{\beta}$, is used.
$$\boldsymbol{\beta} = \mathbf{M} L^{-1} = \sigma^{\frac{1}{2}} \mathbf{B}_0 (\rho\nu)^{\frac{1}{2}}. \tag{12}$$

Now
$$\left.\begin{aligned} \nabla^2 \equiv (h_\phi h_\psi)^{-1}\left\{\frac{\partial}{\partial\phi}\left(\frac{h_\psi}{h_\phi}\frac{\partial}{\partial\phi}\right) + \frac{\partial}{\partial\psi}\left(\frac{h_\phi}{h_\psi}\frac{\partial}{\partial\psi}\right)\right\} \equiv (M/M^*)^2\left\{\frac{\partial^2}{\partial\phi^2} + \frac{\partial^2}{\partial\psi^2}\right\}, \\ (\mathbf{B}_0 . \nabla) \equiv (B_0/h_\phi)\frac{\partial}{\partial\phi} \equiv (B_0^2/B^*)\frac{\partial}{\partial\phi}. \end{aligned}\right\} \tag{13}$$

We can now rewrite equations (6) and (7) in the form

$$\frac{\partial^2 V_z}{\partial\phi^2} + \frac{\partial^2 V_z}{\partial\psi^2} + sM^*\frac{\partial B_z}{\partial\phi} = -\frac{PL^2}{\rho\nu}\left(\frac{M^*}{M}\right)^2 \tag{14}$$

and
$$s\left\{\frac{\partial^2 B_z}{\partial\phi^2} + \frac{\partial^2 B_z}{\partial\psi^2}\right\} + M^*\frac{\partial V_z}{\partial\phi} = 0, \tag{15}$$

where
$$s = \mu^{-1}(\sigma\rho\nu)^{-\frac{1}{2}}. \tag{16}$$

Equations (14) and (15) are only slightly different from those given by Shercliff (1953) for a uniform field. Indeed, *each* of the exact solutions obtained for a uniform applied field is a special case of the corresponding general solution obtained by solving equations (14) and (15). Furthermore, with only reasonable restriction on $M(\phi, \psi)$ all the usual boundary-layer techniques can be applied in the limit of large Hartmann number. Useful, alternative forms of the equations (14) and (15) are

$$\frac{\partial^2 m}{\partial\phi^2} + \frac{\partial^2 m}{\partial\psi^2} + M^*\frac{\partial m}{\partial\phi} = -(M^*/M)^2 = -k(\phi, \psi) \tag{17}$$

and
$$\frac{\partial^2 n}{\partial\phi^2} + \frac{\partial^2 n}{\partial\psi^2} - M^*\frac{\partial n}{\partial\phi} = -k(\phi, \psi), \tag{18}$$

where
$$\left.\begin{matrix} m \\ n \end{matrix}\right\} = (V_z \pm sB_z)(\rho\nu/PL^2). \tag{19}$$

The choice of the reference field value and the reference length requires care. The restriction that there is no neutral point of $\mathbf{B}_0$ within the duct, is imposed.†

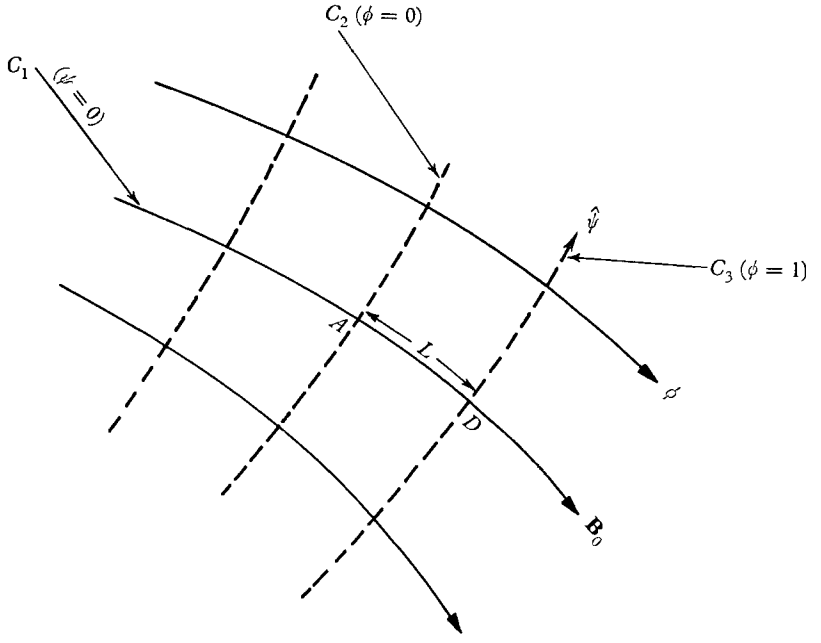

FIGURE 1. The co-ordinate system.

The relevant part of the applied field is depicted in figure 1. The curved field line, C_1, passing through the points A and D is defined as $\psi = 0$. The curve marked C_2 is defined as $\phi = 0$. The value of ϕ at the point D is denoted by ϕ_D. Now

$$\phi_D = \int_0^{\phi_D} d\phi = \oint_0^L (dl/Lh_\phi) = \frac{1}{B^*L}\oint_0^L B_0\, dl,$$

where l measures distance along C_1. Equations (9) and (10) are used in deriving the latter result. In order that B^* be the mean value of B on AD, it is chosen so that $\phi_D = 1$. Thus

$$B^* = (1/L)\oint_0^L B_0(x, y)\, dl. \tag{20}$$

In fact, M^* and β^* are the respective mean values of M and β on AD. ϕ and ψ can now be determined, in terms of x and y, from the equations (9), the equation (20) and the fact that A is the origin of the new co-ordinate system.

The remainder of this paper deals, in detail, with flow through channels with insulating walls. The velocity V_z will be zero at any boundary. In the paragraph below equation (5) it was shown that B_z may be taken as zero at the outer boundary. If there are any inner walls the remarks made in Todd (1967) apply. In

† If there is a neutral point, a more detailed discussion of the (ϕ, ψ) co-ordinate system is required.

§§6 and 7, an annular channel is involved. In these two cases, the remaining boundary conditions are

$$\oint_C \mathbf{E}.\mathbf{dl} = \oint_{C^*} \mathbf{j}.\mathbf{dl} = 0 \quad \text{and} \quad B_z = \text{constant at the inner wall.} \tag{21}$$

C is any closed curve (in the annulus) which surrounds the inner wall. C^* is either of the two boundary curves.

3. Flow at high Hartmann number in insulating ducts of arbitrary cross-section

The topology of the applied transverse magnetic field is just as important as the shape of the duct. To be precise, it is the topology of the duct in (ϕ, ψ) space which matters. Some cases of outstanding interest are discussed below. At the (outer) wall $m = n = 0$ (see §2).

(i) *A duct with a concave boundary*

The region of flow is taken to be simply connected and bounded by a smooth concave curve. This is illustrated in figure 2. The reference curve has been chosen

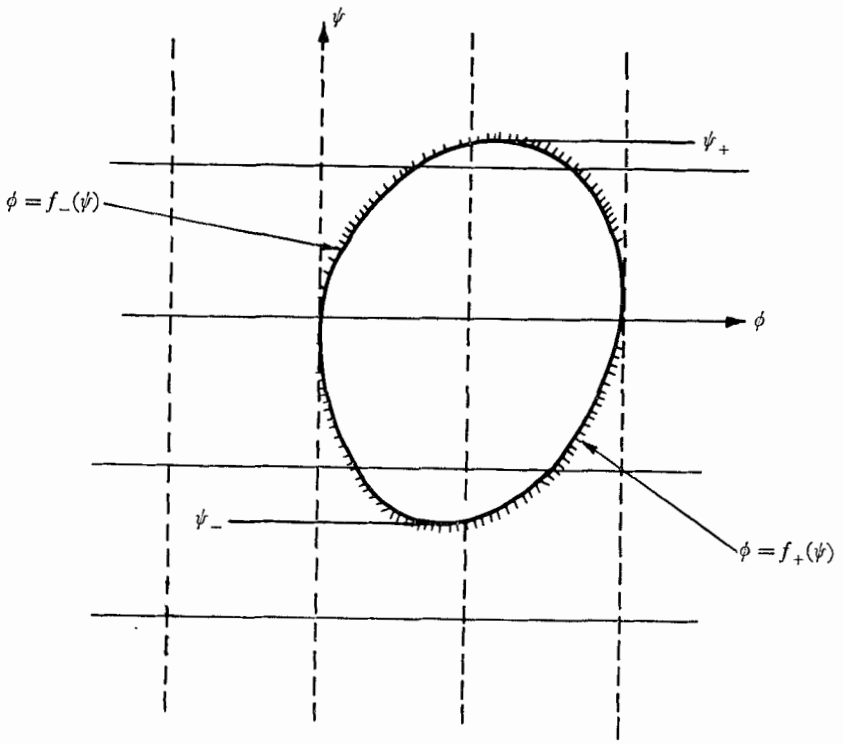

FIGURE 2. A smooth concave duct for which the region of flow is simply connected.

so that $0 \leqslant \phi \leqslant \phi^*$, where ϕ^* is of order one. High Hartmann number means $M^* \gg 1$. In order to apply the usual boundary-layer techniques, the following restrictions are necessary: (i) the first- and second-order partial derivatives of $k(\phi, \psi)$ are not greatly in excess of k; (ii) the first two derivatives of $f_+(\psi)$ and

$f_-(\psi)$ are not greatly in excess of unity, except near $\psi = \psi_+$ and $\psi = \psi_-$. It is a consequence of requirement (i) that k is of order unity where $|\psi|$ is not greatly in excess of one.

A boundary-layer approach shows that m has a boundary layer only on the left-hand side of the duct (i.e. on $\phi = f_-(\psi)$). On the right-hand portion of the wall ($\phi = f_+(\psi)$), m has no boundary layer. Lastly, there is a small obscure region near the point ψ_+ and the point ψ_- (figure 2). A similar result holds for n, left and right being interchanged. Shercliff (1953) was the first to note these features. He gives a full boundary-layer analysis. The typical 'thickness' of these layers in the (ϕ, ψ)-plane is $(M^*|\cos\theta|)^{-1}$, where θ is the angle which the inward normal makes with the ϕ axis. Let ϵ be the corresponding distance in real space then it follows from equations (10) that

$$(M^*|\cos\theta|)^{-1} = (\epsilon M/LM^*) = (\epsilon/Lh_\phi)$$

therefore

$$\epsilon = L(M|\cos\theta|)^{-1} = (\beta|\cos\theta|)^{-1}. \tag{22}$$

The transformation is conformal and so (θ) is still the angle between the (*curved*) field line and the normal to the boundary. This result merely confirms that it is the *local* behaviour of $\mathbf{B}_0$ which is important. Outside the boundary layers and the obscure regions, there is a core flow. It is consistent to seek solutions of the type

$$m_{\text{core}} = m_c = (M^*)^{-1}\mathscr{M}_1(\phi, \psi) + (M^*)^{-2}\mathscr{M}_2(\phi, \psi) + \ldots,$$

and

$$n_{\text{core}} = n_c = (M^*)^{-1}\mathscr{N}_1(\phi, \psi) + (M^*)^{-2}\mathscr{N}_2(\phi, \psi) + \ldots,$$

where the $\mathscr{M}$'s and $\mathscr{N}$'s have values not greatly in excess of $k(\phi, \psi)$. It is found that

$$m_c = (M^*)^{-1}\int_{\phi}^{f_+(\psi)} k(t, \psi)\, dt + O\{m_c(M^*)^{-1}\} \tag{23}$$

and

$$n_c = (M^*)^{-1}\int_{f_-(\psi)}^{\phi} k(t, \psi)\, dt + O\{n_c(M^*)^{-1}\}. \tag{24}$$

In deriving equations (23) and (24), the restrictions detailed in the first paragraph were required. The most interesting feature of the flow can be obtained without invoking the higher order correction terms. It follows from equations (19), (23) and (24), that

$$(V_z)_{\text{core}} = (V_z)_c = (PL^2/2\rho\nu M^*)\int_{f_-(\psi)}^{f_+(\psi)} k(t, \psi)\, dt. \tag{25}$$

It can be immediately concluded that $(V_z)_c$ does not vary *along* magnetic field lines, though it does vary *between* them (i.e. with ψ). This is due to the fact that the applied fields (though curved), strongly resist being stretched. The latter feature could, perhaps, be more easily seen from (7) which becomes simply $(\mathbf{B}_0 . \nabla) V_z = 0$ in the core. To highest order, the flow rate, Q, is given by

$$Q = L^2 \int_{\psi_-}^{\psi_+}\int_{f_-}^{f_+} (V_z)_c\, k(\phi, \psi)\, d\phi\, d\psi. \tag{26}$$

Also.

$$(B_z)_c = (\mu PL/2B^*)\left\{\int_{\phi}^{f_+} k(t, \psi)\, dt - \int_{f_-}^{\phi} k(t, \psi)\, dt\right\}. \tag{27}$$

Obviously, there is a curve,† $\phi = \phi(\psi)$, in the core, on which $(B_z)_c = 0$. The current loops to the right of this are described in a clockwise sense; whereas those

† $\phi(\psi)$ is a single valued function of ψ.

currents on the left, loop in an anticlockwise sense (see figure 5). The actual components of the current density vector, **j**, are obtained from

$$\mu\mathbf{j} = \operatorname{curl}\mathbf{B} = (M/LM^*)\left\{\frac{\partial B_z}{\partial\psi}\hat{\boldsymbol{\phi}} - \frac{\partial B_z}{\partial\phi}\hat{\boldsymbol{\Psi}}\right\} = \mu(j_\phi, j_\psi, 0). \tag{28}$$

Thus
$$(j_\psi)_c = (P/B_0), \tag{29}$$

and
$$(j_\phi)_c = (P/2kB_0)\frac{\partial}{\partial\psi}\left\{\int_\phi^{f_+} k(t,\psi)\,dt - \int_{f_-}^{\phi} k(t,\psi)\,dt\right\}. \tag{30}$$

Equation (29) shows that, to highest order, the Lorentz force balances the pressure gradient at each point in the core. If B_0 does not vary between field lines (see §§5(ii); 7(ii)) and if the duct is symmetric about an axis ϕ = constant, then $j_\phi = 0$. Otherwise j_ϕ will, in general, be non-zero.

(ii) *The 'Horseshoe' duct*

The cross-section of the duct is illustrated in figure 3. An analysis, similar to that of §3(i), reveals that there are three distinct core flows. Todd (1967) gives a full

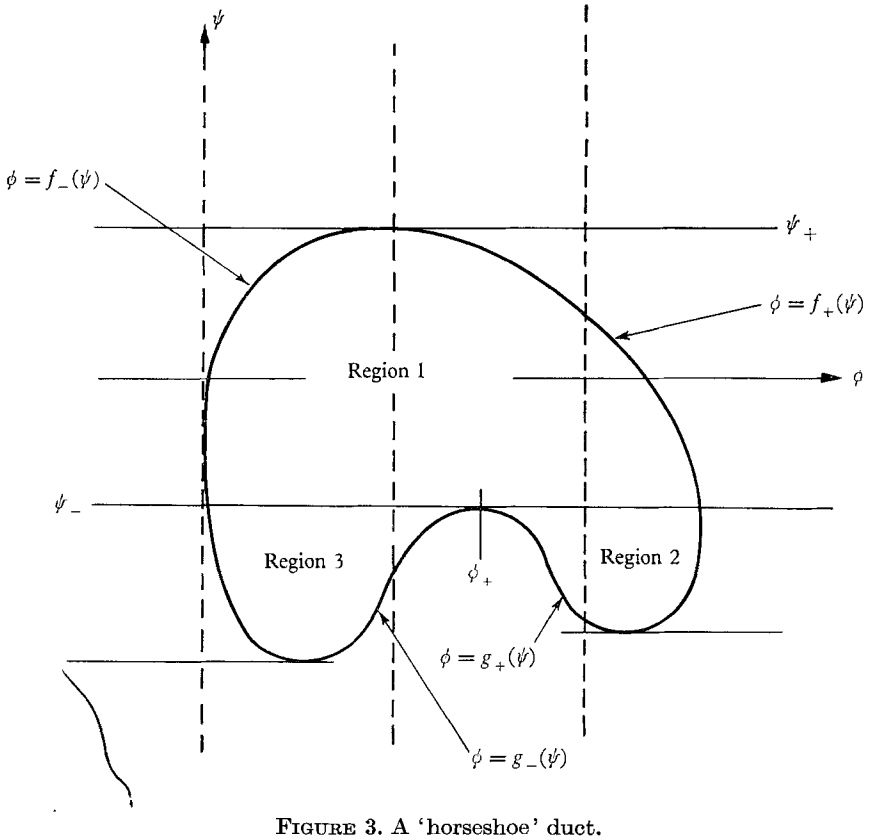

FIGURE 3. A 'horseshoe' duct.

analysis for a uniform applied field. The regions are labelled 1, 2 and 3, as shown in figure 3. In region 1

$$\left.\begin{aligned} m = (m_1)_c &= (M^*)^{-1}\int_\phi^{f_+} k(t,\psi)\,dt \\ \text{and}\quad n = (n_1)_c &= (M^*)^{-1}\int_{f_-}^{\phi} k(t,\psi)\,dt. \end{aligned}\right\} \tag{31}$$

It follows from equations (31) that the values of $(m_1)_c$ and $(n_1)_c$ at $\psi = \psi_-$ are given by

$$M^*(m_1)_c = \int_{\phi}^{f_+(\psi_-)} k(t, \psi_-)\, dt \quad \text{and} \quad M^*(n_1)_c = \int_{f_-(\psi_-)}^{\phi} k(t, \psi_-)\, dt. \tag{32}$$

In region 2

$$m = (m_2)_c = (M^*)^{-1} \int_{\phi}^{f_+} k(t, \psi)\, dt;\ n = (n_2)_c = (M^*)^{-1} \int_{g_+}^{\phi} k(t, \psi)\, dt. \tag{33}$$

Thus at $\psi = \psi_-$

$$(m_1)_c = (m_2)_c; \quad (n_2)_c = (M^*)^{-1} \int_{g_+(\psi_-)}^{\phi} k(t, \psi_-)\, dt \neq (n_1)_c.$$

However,

$$(n_1)_c - (n_2)_c = (M^*)^{-1} \int_{f_-(\psi_-)}^{g_+(\psi_-)} k(t, \psi_-)\, dt = C_1 \,(\text{constant}). \tag{34}$$

This suggests the possibility of a 'wake', or transition layer, centred about $\psi = \psi_-$. (In real space this is a *curved* field line!) Within the wake, it can be assumed that $\partial/\partial\psi \gg \partial/\partial\phi$. Consequently, equation (18) reduces to

$$\frac{\partial^2 n}{\partial \psi^2} - M^* \frac{\partial n}{\partial \phi} = -k(\phi, \psi_-). \tag{35}$$

This equation can be rewritten as

$$\left(\frac{\partial^2}{\partial \psi^2} - M^* \frac{\partial}{\partial \phi}\right)(n - (n_2)_c\{\phi, \psi_-\}) = 0.$$

As in Todd (1967), solutions are sought which are of the (self-similar) form

$$n - (n_2)_c\{\phi, \psi_-\} = F(\alpha), \quad \text{where} \quad \alpha = (M^*)^{\frac{1}{2}}(\psi - \psi_-)/(\phi - \phi_+)^{\frac{1}{2}}. \tag{36}$$

The appropriate boundary conditions are

$$F \to 0 \quad \text{as} \quad \alpha \to -\infty; \quad F \to C_1 \quad \text{as} \quad \alpha \to +\infty.$$

The desired solution is, $$F = \tfrac{1}{2}(C_1)\,(1 + \operatorname{erf}\{\alpha\}). \tag{37}$$

A similar wake for m (but not n) occurs for $\phi < \phi_-$, $\psi = \psi_-$. Of course, m and n are composite physical quantities. Thus, the velocity and induced magnetic field have transition layers ('wakes') on both sides. Some further comments on these 'wakes' are made at the end of the paper. Flow through an annular channel in a uniform field was dealt with in Todd (1967). 'Wakes' of the above type were found to occur. This is also the case for ducts which are annular in (ϕ, ψ) space. Such ducts are necessarily annular in (x, y) space.

(iii) *Other cases*

A pipe whose boundary curve(s) has a *convex* bulge is covered by the first part of this section provided no field line intersects the boundary more than twice. Otherwise, the appropriate analysis is the latter one. Also, it is worth remarking that there is little difficulty if the boundary is piecewise smooth, unless one, or more, piece(s) lies along a field line. This one exceptional case is covered in the next section.

4. Flow in insulating 'Rectangular' ducts

A 'rectangular' duct is one with four sides. One pair of opposite sides lie on the curves $\phi = 0$ and $\phi = 1$, respectively. The other pair of sides have $\psi = 0$ and $\psi = \eta$ (constant), respectively. L is the length AD of the curve $\psi = 0$. B^* is the mean value of B on AD (cf. §2). The exact solutions are obtained by solving the equations (17) and (18), together with the boundary conditions $m = 0 = n$ (cf. last paragraph of §2). The solution for m is

$$m = \exp\{-\tfrac{1}{2}M^*\phi\}\left(\sum_{\iota=1}^{\infty}\left\{A_\iota(M^*,\phi) - \frac{\sinh\alpha_\iota\phi}{\sinh\alpha_\iota}A_\iota(M^*,1)\right\}\sin(\iota\pi\psi/\eta)\right), \quad (38)$$

where

$$\alpha_\iota = 2^{-1}\{(M^*)^2 + 4\iota^2\pi^2\eta^{-2}\}^{\frac{1}{2}} \quad (39)$$

and

$$A_\iota(M^*,\phi) = (-2/\eta\alpha_\iota)\int_0^\eta\int_0^\phi k(t,\psi)\exp\{\tfrac{1}{2}M^*t\}\sinh\alpha_\iota(\phi-t)\sin(\iota\pi\psi/\eta)\,dt\,d\psi. \quad (40)$$

The order of integration in equation (40) can, of course, be reversed. The solution for n is

$$n = \exp\{\tfrac{1}{2}M^*\phi\}\left(\sum_{\iota=1}^{\infty}\left\{A_\iota(-M^*,\phi) - \frac{\sinh\alpha_\iota\phi}{\sinh\alpha_\iota}A_\iota(-M^*,1)\right\}\sin(\iota\pi\psi/\eta)\right). \quad (41)$$

It may be verified that the above solutions reduce to those given by Shercliff (1953) for the case of a uniform, applied field.

At large Hartmann number, the work of §3(i) must apply. (The 'obscure' regions will correspond to a *horizontal* boundary layer on the wall $\psi = 0$ and the wall $\psi = \eta$.) For $M^* \gg 1$,

$$\alpha_\iota = (\tfrac{1}{2}M^*) + O(\iota^2\pi^2/M^*\eta^2). \quad (42)$$

The second term on the right-hand side of equation (42) can be neglected unless it is desired to examine the horizontal boundary layers (for which the high harmonics become important). Thus, α_ι is replaced by $2^{-1}M^*$ in the exact solution. In this approximation,

$$\exp\{-\tfrac{1}{2}M^*\phi\}\left(\sum_{\iota=1}^{\infty}A_\iota(M^*,\phi)\sin(\iota\pi\psi/\eta)\right) = (M^*)^{-1}\int_0^\phi k(t,\psi)\{1-\exp(-M^*(\phi-t))\}dt.$$

The remaining part of the right-hand side of equation (38) reduces to

$$(1-\exp\{-M^*\phi\})\int_0^1 k(t,\psi)\{1-\exp(M^*(t-1))\}\,dt/M^*(1-\exp\{-M^*\}).$$

Thus, to highest order

$$m = (M^*)^{-1}\int_\phi^1 k(t,\psi)\,dt\{1-\exp(-M^*\phi)\}. \quad (43)$$

Equation (39) is in agreement with the results of §3(i). A similar approximation in equation (41) gives

$$n = (M^*)^{-1}\int_0^\phi k(t,\psi)\,dt\{1-\exp(-M^*(1-\phi))\}. \quad (44)$$

It is interesting to note that Shercliff (1953) had to include the highest correction term in equation (42) in order to obtain the corresponding result for a uniform field. This is a comment on the operations which one uses to evaluate *explicitly* the coefficients of the Fourier series. In this limit of large Hartmann number, the following results are valid away from the boundaries (cf. §3(i)):

$$(V_z)_c = (PL^2/2\rho\nu M^*)\int_0^1 k(t,\psi)\,dt, \tag{45}$$

$$(B_z)_c = (\mu PL/2B^*)\left\{\int_\phi^1 k(t,\psi)\,dt - \int_0^\phi k(t,\psi)\,dt\right\}. \tag{46}$$

There will be two sets of current loops as described below equation (27). From (30), it can be deduced that

$$(j_\phi)_c = \{P/2B_0 k(\phi,\psi)\}\left\{\int_\phi^1 - \int_0^\phi\right\}\frac{\partial k(t,\psi)}{\partial\psi}\,dt. \tag{47}$$

If there is variation of B_0 between field lines, $\partial k/\partial\psi \neq 0$. In such cases a non-zero $(j_\phi)_c$ is needed to adjust $(j_\psi)_c$ so that $(j_\psi)_c = PB_0^{-1}$ everywhere in the core. This means that some current lines come out of the Hartmann boundary layers and then rejoin the same boundary layer (see figure 5). If B_0 does not vary between field lines, this effect is not present and $(j_\phi)_c = 0$. The two specific examples given in §§5(i) and (ii) illustrate the former and latter features, respectively.

The boundary layers on the 'horizontal' side walls ($\psi = 0, \psi = \eta$) can be analysed. As shown by Shercliff (1953), these are thicker and of a different nature than the Hartmann boundary layers on the vertical walls ($\phi = 0, 1$). The variables m and n are again employed. It is reasonable to assume that, in this region, $\partial/\partial\psi \gg \partial/\partial\phi$. The case for m at the bottom boundary ($\psi = 0$) will be discussed in detail. The results for n, and for $\psi = \eta$ can then be inferred. Equation (17) is approximated by

$$\frac{\partial^2 m}{\partial\psi^2} + M^*\frac{\partial m}{\partial\phi} = -k(\phi,0). \tag{48}$$

The singular points of $k(\phi,\psi)$ are those of the applied magnetic field. In order to proceed, it will have to be assumed that these (points) are such that the radius of convergence of the series expansion for $k(\phi,0)$ about $\phi = 1$ is greater than unity. Let this series expansion be

$$k(\phi,0) = \sum_{\iota=0}^{\infty} d_\iota(1-\phi)^\iota. \tag{49}$$

By virtue of the above remarks, the series (49) can be integrated and differentiated term by term. This holds for any number of differentiations. It follows that

$$M^* m_c(\phi,0) = \sum_{\iota=0}^{\infty}\{d_\iota(1-\phi)^{\iota+1}/(\iota+1)\}.$$

The required boundary-layer variable, ξ, is defined as

$$\xi = \{\tfrac{1}{4}M^*\psi^2/(1-\phi)\}. \tag{50}$$

A solution, valid in the layer, is sought in the form

$$M^* m = \sum_{\iota=0}^{\infty}(1-\phi)^{\iota+1}d_\iota\{(\iota+1)^{-1} - G_{\iota+1}(\xi)\}. \tag{51}$$

The lower edge of the boundary layer is achieved as $\xi \to \infty$. In this limit, each of the G_ι will be required to vanish. This ensures that $m \to m_c$. At the wall, $m = 0$ and so it is required that

$$G_\iota(0) = (\iota)^{-1}. \tag{52}$$

The (convergence) properties of the series (51) are assumed to be similar to those of the series (49). The equation (48) is satisfied if

$$\xi \frac{d^2G_\iota}{d\xi^2} + (2^{-1} + \xi)\frac{dG_\iota}{d\xi} - \iota G_\iota = 0, \tag{53}$$

for all the relevant values of ι. Equation (53) is the confluent hypergeometric equation with the independent variable $(-\xi)$. There are many ways in which the desired solution can be presented. For example, one solution is a polynomial of degree ι. Thus for $\iota = 1$, the desired solution can very easily be found by reduction of order (see Shercliff 1953). The general solution is

$$G_\iota = (1/\iota)F(-\iota|(\tfrac{1}{2})|-\xi) - \{(\iota-1)!\,2\}\{\Gamma(\iota+(\tfrac{1}{2}))\}^{-1}\xi^{\frac{1}{2}}F(-\iota+(\tfrac{1}{2})|(\tfrac{3}{2})|-\xi), \tag{54}$$

where F is the confluent hypergeometric function. In fact G_ι is just a multiple of $U_1(-\iota|\frac{1}{2}|-\xi)$, which is a confluent hypergeometric function of the third kind. U_1 is fully discussed in Morse & Feshbach (1953). As $\xi \to \infty$,

$$|G_\iota| \sim (\xi)^{-\iota-(\frac{1}{2})}\exp\{-\xi\}. \tag{55}$$

In a paper on singular perturbation problems, Eckhaus & de Jager (1966) show that the solution to the above boundary-layer problem can also be given in the form

$$m = -\left(\frac{2}{\pi}\right)^{\frac{1}{2}}\int_{\psi(2M^*(1-\phi))^{-\frac{1}{2}}}^{\infty}(\exp\{-\tfrac{1}{2}t^2\})\, m_c(\phi + \frac{\psi^2}{2M^*t^2}, 0)\, dt + m_c(\phi, 0).$$

This form may sometimes be more convenient than (51), which is a series expansion of it. (The series solution was employed in the detailed calculations of §5(ii).) A similar analysis holds for n in the boundary layer on $\psi = 0$. The result is

$$\begin{aligned} n &= -(2/\pi)^{\frac{1}{2}}\int_{\psi(2M^*\phi)^{-\frac{1}{2}}}^{\infty}\{\exp(-\tfrac{1}{2}t^2)\}\, n_c(\phi - \frac{\psi^2}{2M^*t^2}, 0)\, dt + n_c(\phi, 0) \\ &= \sum_{\iota=0}^{\infty}(M^*)^{-1}e_\iota\phi^{\iota+1}\{(\iota+1)^{-1} - G_{\iota+1}(\zeta)\}, \end{aligned} \tag{56}$$

where

$$k(\phi, 0) = \sum_{\iota=0}^{\infty} e_\iota\phi^\iota \quad \text{and} \quad \zeta = (\psi^2M^*/4\phi).$$

The analysis for the boundary layer on $\psi = \eta$ is identical except that $(\eta - \psi)$ takes the place of ψ in the definitions of the boundary-layer variables and $k(\phi, \eta)$ is used instead of $k(\phi, 0)$. The above results show that m and n, the composite variables, have broadening boundary layers, the thickness tending to zero at the end where the core value is zero. The real physical quantities have a boundary layer of more or less uniform thickness. The typical thickness of the layer on $\psi = 0$, ϵ_0 (say), is given by

$$\epsilon_0 = L^{\frac{1}{2}}(\beta^*)^{-\frac{1}{2}}. \tag{57}$$

The latter result may be deduced from equations (9), (10), (50) and (51). L is the length of the boundary $\psi = 0$ and β^* the average value of β on it. In a similar way, it can be shown that the typical thickness of the layer on $\psi = \eta$, ϵ_η (say), is given by

$$\epsilon_\eta = L_\eta^{\frac{1}{2}}(\beta_\eta^*)^{-\frac{1}{2}}, \tag{58}$$

where L_η is the length of the boundary $\psi = \eta$ and β_η^* is the mean value of β on it. The latter result is in agreement with the fact that the actual choice of the reference field line is of no physical significance. The first four boundary-layer

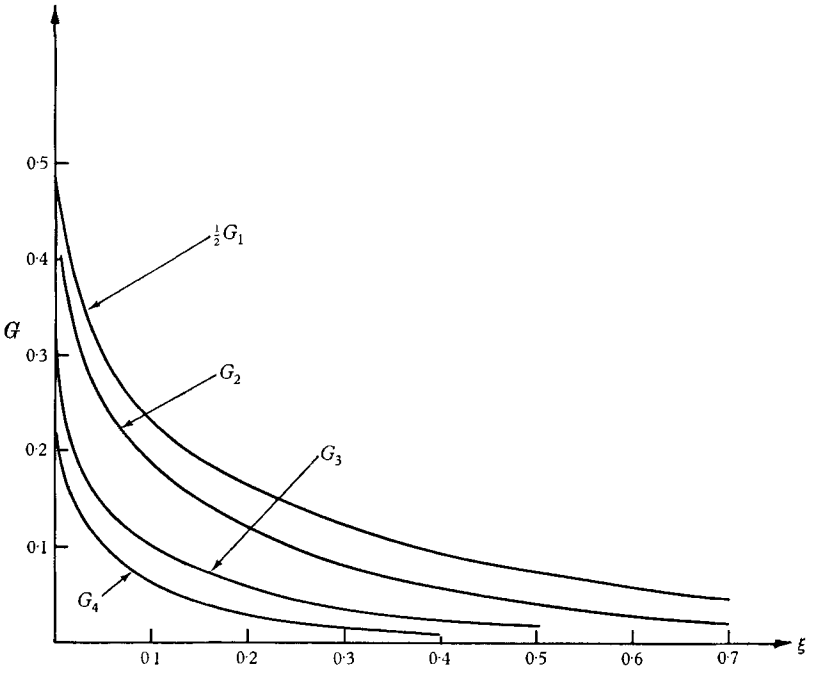

FIGURE 4. The first four boundary-layer functions.

functions are plotted in figure 4. Shercliff (1953) plotted G_1 against $\{2(\xi)^{\frac{1}{2}}\}$. It seems possible that these side boundary layers might have points of inflexion in some cases. This is not found for the problem discussed in §5(ii).

5. Two applications of the theory for rectangular ducts

A circular field and a radial field are considered. These fields have special features and the results for them, together with the general theory, provide an ample understanding of flows within rectangular ducts.

(i) *A circular field*

$$\boldsymbol{\beta} = (C/r)\hat{\boldsymbol{\theta}}, \tag{59}$$

where C is a positive† constant and (r, θ) are plane polar co-ordinates. The above field can be created by a line current, although the current-carrying conductor would have to be sheathed in an insulator to let $E_z = 0$, outside. The rectangular duct is defined by $0 < \theta < \theta_0$; $a\delta < r < a$. The typical length is chosen to be

† The results for $C < 0$, follow from those for $\boldsymbol{\beta} = \{|C|/r\}\,\hat{\boldsymbol{\theta}}$; the only change being the reversal of all currents.

$(a\theta_0)$. $\phi = 0 = \psi$ corresponds to $r = a$, $\theta = 0$. Thus

$$\phi = (\theta/\theta_0), \quad \psi = (-1/\theta_0)\log(r/a) \quad \text{and} \quad \eta = (-1/\theta_0)\log(\delta). \tag{60}$$

Also,
$$a\theta_0\beta^* = M^* = C\theta_0, \quad k = \exp\{-2\theta_0\psi\}. \tag{61}$$

The analysis of §4 gives the following results for the limit of high Hartmann number:

$$\left.\begin{aligned} (V_z)_c &= (P\theta_0^2 r^2/2\rho\nu M^*), \\ (B_z)_c &= \mu Pr(\theta_0 - 2\theta)/2B_0, \\ (j_\theta)_c &= (j_\phi)_c = P(2\theta - \theta_0)/2B_0, \\ \text{and} \quad -(j_r)_c &= (j_\psi)_c = (P/B_0). \end{aligned}\right\} \tag{62}$$

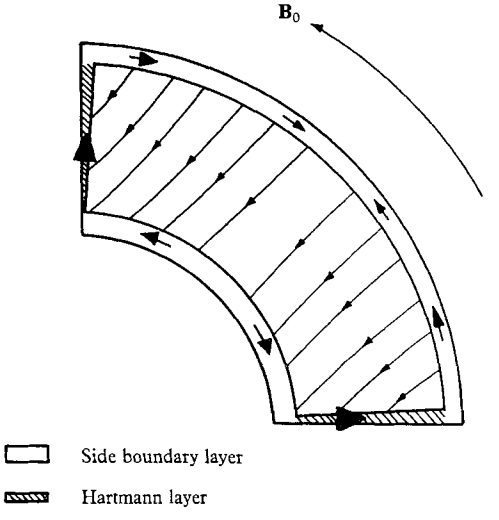

FIGURE 5. Current flow for a 'rectangular' duct in a circular field.

The core current paths are illustrated in figure 5, for which θ_0 was taken as $(\frac{1}{2}\pi)$ and $\delta = \frac{1}{2}$. The Hartmann boundary layers have a typical thickness (r/C). This corresponds to the fact that B_0 varies inversely with r. In the side boundary layer at $r = a$,

$$m = (1-\phi)\{1 - G_1(\xi)\}(M^*)^{-1}$$

and
$$n = \phi\{1 - G_1(\zeta)\}(M^*)^{-1}.$$

Thus only G_1 is needed. This happens only for circular and uniform fields, which have the property, $\mathbf{B}_0 = B_0(\psi)\,\hat{\boldsymbol{\phi}}$. In all other cases, the hierarchy of boundary-layer functions are needed. The boundary-layer profiles of V_z, at $\phi = \frac{1}{4}$ and $\frac{1}{2}$, are given in figure 6. $V_z(\phi, \psi)$ is symmetric about $\phi = (\frac{1}{2})$. The typical thickness of the side boundary layer at $r = a$ is $a(\theta_0/C)^{\frac{1}{2}}$. For the layer at $r = a\delta$, the thickness is $a(\theta_0\delta/C)^{\frac{1}{2}}$. To highest order, the flow rate, Q, is given by

$$Q = \{Pa^4\theta_0^3(1-\delta^4)/8M^*\rho\nu\}. \tag{63}$$

Lastly, it is worth remarking that the high Hartmann number analysis applies however close δ is to zero. This is a consequence of the fact that

$$\delta\{B_0(a\delta)\} = \text{constant, independent of } \delta.$$

(ii) *A radial field*

$$\boldsymbol{\beta} = (D/r)\,\hat{\mathbf{r}}, \tag{64}$$

where D is a positive† constant. The duct is defined by $0 \leqslant \theta \leqslant \theta_0$ and $a\delta \leqslant r \leqslant a$. The typical length is $a(1-\delta)$ and the point $\phi = 0 = \psi$ corresponds to $r = a\delta$, $\theta = 0$. A good approximation to this radial field can be obtained by suitably

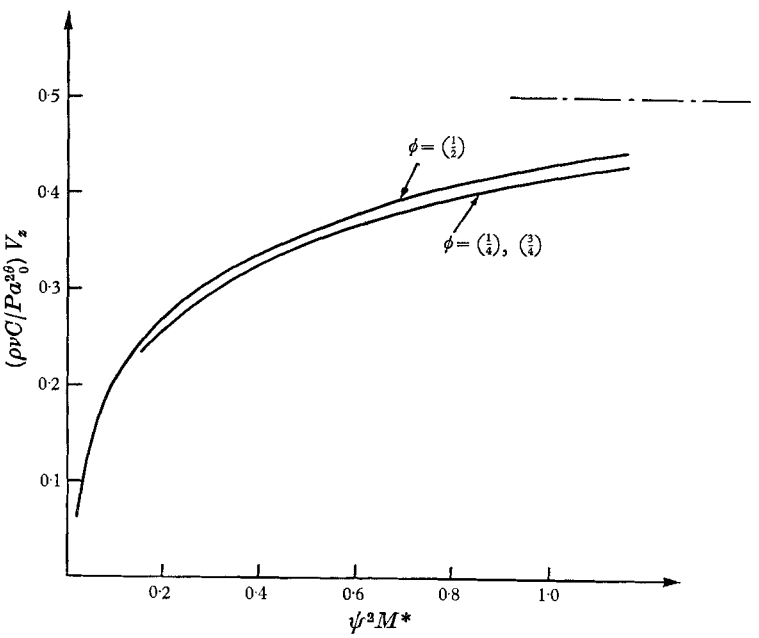

FIGURE 6. Some profiles of V_z in the side boundary layers ($\mathbf{B}_0$ circular).

placed cylindrical pole pieces. Now

$$\phi = \gamma^{-1}\log(r/a\delta), \quad \psi = \gamma^{-1}\theta \quad \text{and} \quad \eta = \gamma^{-1}\theta_0, \quad \text{where} \quad \gamma = \log(1/\delta).$$

Also, $$a(1-\delta)\beta^* = M^* = \gamma D \quad \text{and} \quad k = (\gamma\delta/1-\delta)^2\exp\{2\gamma\phi\}. \tag{65}$$

The analysis of §4, which deals with the flow in the limit of high Hartmann number, gives the following results:

$$\left.\begin{aligned} (V_z)_c &= Pa^2(1-\delta^2)/4\rho\nu D = \text{constant}, \\ (j_\psi)_c &= (j_\theta)_c = (P/B_0); \quad j_\phi = j_r = 0, \\ m_c &= \gamma\{1-\delta^2\exp(2\gamma\phi)\}/2M^*(1-\delta)^2 \\ \text{and} \qquad n_c &= \gamma\delta^2\{\exp(2\gamma\phi)-1\}/2M^*(1-\delta)^2. \end{aligned}\right\} \tag{66}$$

The typical thickness of the Hartmann layer on $r = a\delta$ is $(a\delta/D)$. On $r = a$, the thickness is (a/D). In neither case, is there any dependence on θ. In the side

† See remarks below equation (59).

boundary layers the equations (51), (54) and (56) apply with

$$d_\iota = \{\gamma^2(-2\gamma)^\iota/(1-\delta)^2(\iota!)\} = (-)^\iota \delta^{-2} e_\iota. \tag{67}$$

The layer on $\theta = \theta_0$ is identical with that on $\theta = 0$. Figure 7 shows the profiles of V_z at $\phi = \frac{1}{4}, \frac{1}{2}$ and $\frac{3}{4}$, for the case $\theta_0 = (\frac{1}{2}\pi)$ and $\delta = \frac{1}{2}$. The typical thickness of these layers is $a(1-\delta)(\gamma D)^{-\frac{1}{2}}$. The applied magnetic field described in this section has the property $B_0 = B_0(\phi)\hat{\boldsymbol{\phi}}$. The only other field with this property is the uniform one. In these two cases, $j_\phi = 0$ for a duct symmetric about an axis $\phi =$ constant (see § 3).

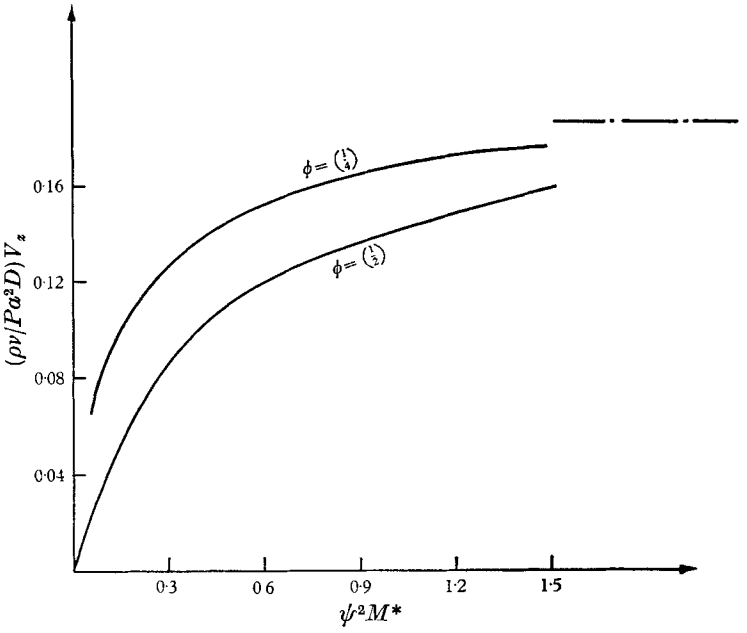

FIGURE 7. Some profiles of V_z in the side boundary layers for a radial field. (The profile of V_z at $\phi = \frac{3}{4}$ is not significantly different from that for $\phi = \frac{1}{4}$.)

6. Another flow across an azimuthal, transverse field

In some situations the applied magnetic field lines are closed loops. This is the case for a circular field (§ 5(i)). It also occurs if two adjacent line currents are in opposition. The type of duct to be considered is drawn in figure 8. The inner boundary coincides with a field line. So does the outer wall, which is taken as $\psi = 0$, the reference curve. The equipotential, $\phi = 0$, need not be explicitly defined. At the inner wall, $\psi = \eta$. The governing equations are (17) and (18). At the outer boundary, $m = n = 0$ (see § 2). The usual periodicity conditions apply between $\phi = 0$ and $\phi = 1$. The conditions at the inner boundary need more careful consideration. The induced electric field, $\mathbf{V} \wedge \mathbf{B}$, has no ϕ component. Thus it follows from equation (3) that at all points

$$E_\phi = \sigma^{-1} j_\phi. \tag{68}$$

The boundary condition (21) can now be applied. This can be reduced to

$$\int_0^1 j_\phi h_\phi L d\phi = 0, \quad \text{for any fixed value of } \psi. \tag{69}$$

But no source of current exists and so†

$$\int_0^\eta j_\phi h_\psi L d\psi = I = \text{constant}, \tag{70}$$

therefore
$$I = \int_0^1 \int_0^\eta j_\phi h_\psi L d\psi d\phi = \int_0^\eta \int_0^1 j_\phi h_\phi L d\phi d\psi = 0. \tag{71}$$

This means that $m = n = 0$ at the inner boundary.†

The exact solution to the problem is

$$m = \sum_{\iota=1}^{\infty} \left\{ I_0(\alpha_\iota, \phi) - I_0(-\alpha_\iota, \phi) - \frac{I_0(\alpha_\iota, 1) \exp\{(\alpha_\iota - (\tfrac{1}{2}M^*)\phi\}}{\exp\{\alpha_\iota - (\tfrac{1}{2}M^*)\} - 1} + \frac{I_0(-\alpha_\iota, 1) \exp\{(-\alpha_\iota - (\tfrac{1}{2}M^*))\phi\}}{\exp\{-\alpha_\iota - (\tfrac{1}{2}M^*)\} - 1} \right\} \sin(\iota\pi\psi/\eta), \tag{72}$$

where

$$I_0(\alpha_\iota, \phi) = -\int_0^\phi \exp\{(\alpha_\iota - (\tfrac{1}{2}M^*))(\phi - t)\} \int_0^\eta \{k(t, \psi)/\eta\alpha_\iota\} \sin(\iota\pi\psi/\eta)\, d\psi\, dt. \tag{73}$$

The other composite variable, n, can be obtained from equations (72) and (73) by replacing M^* with $(-M^*)$ (cf. equations (17), (18), (38) and (42)). Once again the high Hartmann number limit is examined. It is desirable to obtain the first two terms in the expansion for m. Thus, α_ι is approximated by

$$\alpha_\iota = (\tfrac{1}{2}M^*) + (\iota^2\pi^2/\eta^2 M^*) + (\text{negligible terms}). \tag{74}$$

A procedure very similar to that described in the first part of §4, gives

$$m_c = \mathscr{M}_0(\psi) + \mathscr{M}_1(\phi, \psi)(M^*)^{-1} + \ldots, \tag{75}$$

where
$$\mathscr{M}_0 = \int_0^1 \left\{ (\psi/\eta) \int_0^\eta - \int_0^\psi \right\} \int_0^p k(t, r)\, dr\, dp\, dt \tag{76}$$

and
$$\mathscr{M}_1 = \left\{ \phi \int_0^1 - \int_0^\phi + \int_0^1 \{(\tfrac{1}{2}) - t\} \right\} k(t, \psi)\, dt. \tag{77}$$

The periodicity boundary conditions are satisfied. $\mathscr{M}_0$ is zero at $\psi = 0, \eta$ but $\mathscr{M}_1$ is not, thus there will be the expected boundary layers on $\psi = 0, \eta$. In these layers the neglected higher harmonics are important. A similar procedure with the exact solution for n, yields

$$n_c = \mathscr{M}_0 - \mathscr{M}_1(M^*)^{-1} + \ldots. \tag{78}$$

The latter result is not obvious.

It is instructive to derive the results (75) and (78) using the approach employed in §3. This gives

$$\frac{d^2\mathscr{M}_0}{d\psi^2} + \frac{\partial \mathscr{M}_1}{\partial \phi} = -k(\phi, \psi). \tag{79}$$

The latter equation can be integrated with respect to ϕ between the limits 0 and 1. If the fact that $\mathscr{M}_1$ is periodic in ϕ is then introduced, the result (76) is obtained

† See, for example, Todd (1967).

upon the further requirement that $\mathscr{M}_0(\psi)$ is zero at $\psi = 0$ and $\psi = \eta$. The latter restriction is consistent with the fact that $\mathscr{M}_0(\psi)$ does not exhibit boundary-layer behaviour near $\psi = 0$ and $\psi = \eta$. The expression (76) for $\mathscr{M}_0$ can be substituted in equation (79). The resultant equation is

$$\frac{\partial \mathscr{M}_1}{\partial \phi} = k_a - k, \tag{80}$$

where

$$k_a = \int_0^1 k(t, \psi)\, dt. \tag{81}$$

k_a is the average value of k on $\psi =$ constant. It is worth noting that, as k is periodic in ϕ, equation (80) shows that all the derivatives of $\mathscr{M}_1$ have this periodicity. Equation (80) gives

$$\mathscr{M}_1 = \phi k_a - \int_0^{\phi} k(t, \psi)\, dt + F(\psi),$$

where $F(\psi)$ is an unknown function of ψ.

Consideration of the variation of $\mathscr{M}_1$ within the boundary layers shows that

$$\int_0^1 \mathscr{M} d\phi = 0.$$

The application of this latter condition reveals that $\mathscr{M}_1$ is defined by equation (77). The full results are

$$(V_z)_c = (P/\rho\nu)\int_0^1 \left\{(\psi/\eta)\int_0^{\eta} - \int_0^{\psi}\right\}\int_0^p \frac{(B^*L)^2}{B_0^2}\, dr\, dp\, dt + o\{(V_z)_c (M^*)^{-2}\}, \tag{82}$$

$$(B_z)_c = \mu P\left\{\phi\int_0^1 - \int_0^{\phi} + \int_0^1 (\tfrac{1}{2} - t)\right\}\frac{B^*L}{B_0^2}\, dt + o\{(B_z)_c (M^*)^{-1}\}. \tag{83}$$

The corresponding components of the current density vector are

$$(j_\psi)_c = \frac{P}{B_0}\left\{1 - \frac{k_a}{k}\right\} \tag{84}$$

and

$$(j_\phi)_c = \frac{P}{B_0 k}\frac{\partial \mathscr{M}_1}{\partial \psi}. \tag{85}$$

Equation (82) shows that the core velocity remains of the same order as for the case $B_0 = 0$! However, $(V_z)_c$ is flattened in the sense that it does not vary with ϕ. The latter result is usual in Hartmann flows (§ 3) but the former is quite novel. The charge separation between the walls creates an electric field which, to highest order, balances the induced one. The current paths are very interesting (and involved). For each ψ, k must assume its mean value, k_a, an even number of times. Also, the average value of $\partial \mathscr{M}_1/\partial\psi$ on a curve $\psi =$ constant, is zero. Thus, $(j_\phi)_c$ will be zero an even number of times for each ψ. A typical current pattern is shown in figure 8. (In drawing this qualitative diagram it was assumed that 2 was the appropriate even number.)

Since $\mathscr{M}_1$ does not vanish either at $\psi = 0$ or at $\psi = \eta$, there will be boundary layers. Let

$$m = \mathscr{M}_0(\psi) + (M^*)^{-1}\{\mathscr{M}_1(\phi, 0) - U\} + \ldots, \tag{86}$$

in the layer at $\psi = 0$. The governing equation for U is

$$\frac{\partial^2 U}{\partial \omega^2} + \frac{\partial U}{\partial \phi} = 0, \tag{87}$$

where

$$\omega = (M^*)^{-\frac{1}{2}} \psi. \tag{88}$$

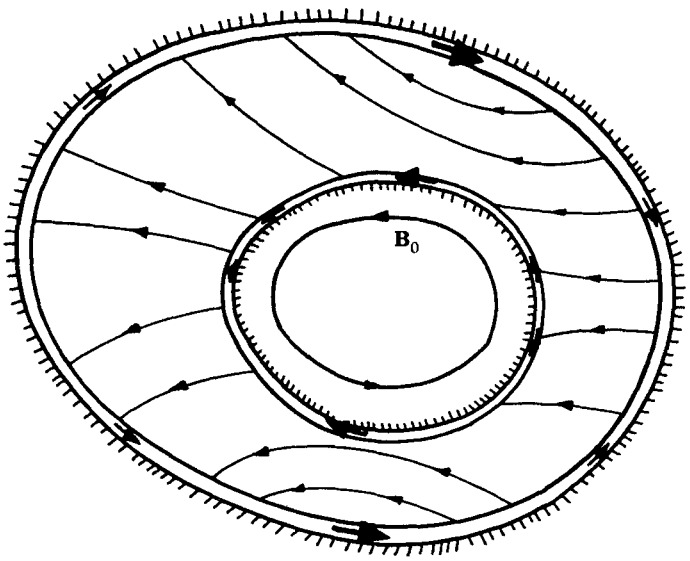

FIGURE 8. The (qualitative) current paths (§6).

It has been assumed that $\partial/\partial\psi \gg \partial/\partial\phi$. The boundary conditions are that

$$\left.\begin{aligned} U &= \mathscr{M}_1(\phi, 0) \quad \text{at} \quad \omega = 0 \\ \text{and} \qquad U &\to 0 \quad \text{as} \quad \omega \to \infty. \end{aligned}\right\} \tag{89}$$

The problem is solved in terms of the complete Fourier series.

$$\left.\begin{aligned} U = \sum_{\iota=1}^{\infty} A_\iota \exp\{-(\iota\pi)^{\frac{1}{2}}\omega\} \sin\{(\iota\pi)^{\frac{1}{2}}\omega + 2\iota\pi\phi\} \\ + \sum_{\iota=1}^{\infty} C_\iota \exp\{-(\iota\pi)^{\frac{1}{2}} w\} \cos\{(\iota\pi)^{\frac{1}{2}} w + 2\iota\pi\phi\}, \end{aligned}\right\} \tag{90}$$

where

$$\left.\begin{aligned} A_\iota &= 2\int_0^1 \mathscr{M}_1(t, 0) \sin(2\iota\pi t)\, dt \\ \text{and} \qquad C_\iota &= 2\int_0^1 \mathscr{M}_1(t, 0) \cos(2\iota\pi t)\, dt. \end{aligned}\right\} \tag{91}$$

Let

$$n = \mathscr{M}_0(\psi) - (M^*)^{-1}\{\mathscr{M}_1(\phi, 0) - V\} \tag{92}$$

in the layer on $\psi = 0$. The result for V is obtained by substituting $(1-\phi)$ for ϕ in the equations (90); and $\mathscr{M}_1\,(1-t, 0)$ for $\mathscr{M}_1\,(t, 0)$ in the equations (91). The physical variables are given by

$$\{\rho\nu(V_z)/PL^2\} = \mathscr{M}_0(\psi) - (2/M^*) \times \sum_{\iota=1}^{\infty} \exp\{-(\iota\pi)^{\frac{1}{2}}\omega\} \sin\{(\iota\pi)^{\frac{1}{2}}\omega\} \int_0^1 \mathscr{M}_1(t, 0) \sin\{2\iota\pi(t-\phi)\}\, dt, \tag{93}$$

$$\{\rho\nu s B_z/PL^2\} = (M^*)^{-1}\mathscr{M}_1(\phi,\psi) - (2/M^*) \times \sum_{\iota=1}^{\infty} \exp\{-(\iota\pi)^{\frac{1}{2}} w\}\cos\{(\iota\pi)^{\frac{1}{2}} w\}\int_0^1 \mathscr{M}_1(t,0)\cos\{2\iota\pi(t-\phi)\}\,dt. \quad (94)$$

The first result shows that the velocity rises from zero to order $(M^*)^{-\frac{1}{2}}\,(V_z)_c$ across the boundary layer. The corresponding results for the boundary layer on $\psi = \eta$ are obtained by replacing ψ by $(\eta - \psi)$ and $\mathscr{M}_1(\phi, 0)$ by $\mathscr{M}_1(\phi, \eta)$ in the above discussion. The typical boundary-layer thicknesses are those given by equations (57) and (58).

The case of the field due to a line current,

$$\boldsymbol{\beta} = (C/r)\,\hat{\boldsymbol{\theta}}, \quad (95)$$

is rather special. If the boundaries are the concentric circles: $r = a\delta$ and $r = a$, the exact solution is

$$\left.\begin{aligned} B_z &= 0, \\ V_z &= (P/4\rho\nu)\{(a^2\delta^2 - r^2) + a^2(1-\delta^2)\log(r/a\delta)\{\log\delta\}^{-1}\} \\ \text{and} \quad \mathbf{E} &= -\{V_z(r)\,B_0(r)\}\,\hat{\mathbf{r}}. \end{aligned}\right\} \quad (96)$$

The flow is unaffected by the magnetic field. The reason is essentially that in this case curl $(\mathbf{v}\wedge\mathbf{B}_0) = 0$ so that no currents are induced by the motion (e.g. Shercliff 1965). Note that $B_0 = B_0(\psi)$ in this case, as in the case of a uniform field. No other field has this property, so that in every other case, the core flow will be as described below equation (85), and a boundary layer will be present.

7. Another flow in a radial-type field

Whenever an annular channel encloses a cylindrical pole piece, each magnetic field line will intersect the inner and outer boundary just once. Some discussion on the experimental aspects of such flows are given in § 7 (ii). If the inner and outer boundaries coincide with equiponential curves, the exact solution can easily be obtained. It is this situation which is now considered. The reference curve, $\psi = 0$, need not be explicitly defined. The applied field will be taken as pointing outwards, i.e. from the inner to the outer wall. If the applied field points inwards, ϕ should be replaced by $(1-\phi)$ in the subsequent discussion. The boundary conditions (see § 2) are

$$V_z = 0 \quad \text{at} \quad \phi = 0, 1; \quad B_z = 0 \quad \text{at} \quad \phi = 1;$$

$$\{\rho\nu s B_z/PL^2\} = (A/M^*) = \text{constant} \quad \text{at} \quad \phi = 0;$$

and

$$\oint_{C_1} \mathbf{E}.\mathbf{dl} = 0,$$

where C_1 is any closed loop within the duct.

As always, many interesting features can be uncovered by a boundary-layer analysis in the limit of high Hartmann number (see § 3). The results are

$$M^* m = \int_\phi^1 k(t,\psi)\,dt(1-\exp\{-M^*\phi\}) + A\exp\{-M^*\phi\} + O(m) \quad (97)$$

and

$$M^* n = \left\{\int_0^\phi k(t,\psi)\,dt - A\right\}(1-\exp\{-M^*(1-\phi)\}) + O(n). \quad (98)$$

Thus
$$(V_z)_c = \{k_a - A\} PL^2/2\rho\nu M^*$$

and
$$\rho\nu s(B_z)_c = (PL^2/2M^*)\left\{A + \left(\int_\phi^1 - \int_0^\phi\right) k(t,\psi)\,dt\right\}.$$

The last mentioned boundary condition can now be applied. It requires that

$$A(1+O\{(M^*)^{-1}\}) = \eta^{-1}\int_0^\eta\int_0^1 k(\phi,\psi)\,d\phi\,d\psi = \bar{k}. \tag{99}$$

$\bar{k}$ is the mean value of k within the duct. $\bar{k}$ is also the mean value of $k_a(\psi)$. It follows that

$$(V_z)_c = (PL^2/2\rho\nu M^*)\,(k_a - \bar{k}), \tag{100}$$

$$(B_z)_c = (\mu PL/2B^*)\left\{\bar{k} + \left(\int_\phi^1 - \int_0^\phi\right) k(t,\psi)\,dt\right\}, \tag{101}$$

$$(j_\psi)_c = (P/B_0) \tag{102}$$

and
$$(j_\phi)_c = (P/2B_0 k)\left\{\int_\phi^1 - \int_0^\phi\right\}\frac{\partial k}{\partial\psi}(t,\psi)\,dt. \tag{103}$$

The first of these results means that if B_0 varies with ψ, the core velocity will be negative in parts of the duct! As usual, the core velocity varies only in the

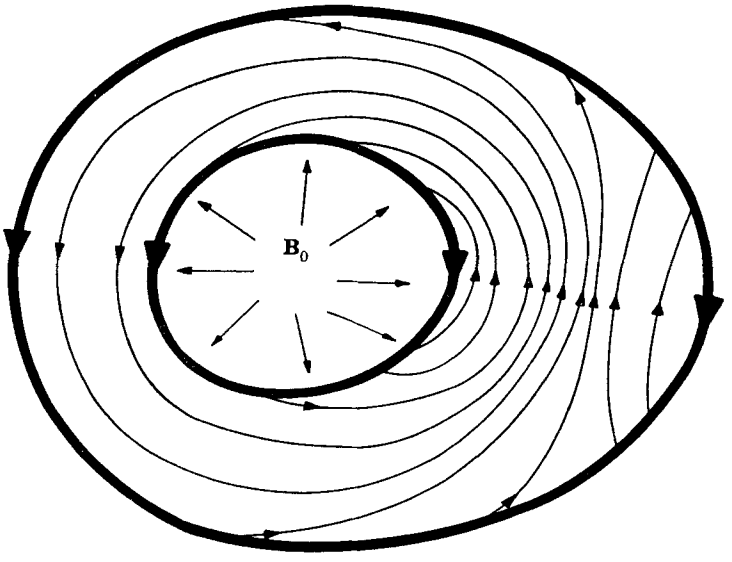

FIGURE 9. The (qualitative) current paths (§7).

direction normal to the magnetic field lines, i.e. vorticity perpendicular to $\mathbf{B}_0$ is suppressed. The mean value of $(V_z)_c$ is of order $\bar{V}(M^*)^{-1}$, where $\bar{V}$ is the mean value of $|(V_z)_c|$. The current path lines can be sketched with the aid of equations (99) to (103) and the knowledge that Hartmann boundary layers exist on the walls. The qualitative features of the current flow are sketched† in figure 9.

† k_a is assumed to take the value $\bar{k}$ at two values of ψ. Also, $\partial k/\partial\psi$ is assumed to be zero at two values of ψ for each ϕ.

(i) *A radial field*

$$\boldsymbol{\beta} = (D/r)\,\hat{\mathbf{r}}.$$

The sides of the duct are circular with radius $a\delta$ and a. Globe (1959) has derived the exact solution. The results in the present notation (and correcting an error in Globe's expression for B_z) are

$$V_z = \{Pa^2\delta^2/\rho\nu(D^2-4)\}\,[(r/a\delta)^2 + \frac{\sinh\{D\ln(r/a)\} - \delta^{-2}\sinh\{D\ln(r/a\delta)\}]}{\sinh M^*} \tag{104}$$

and

$$B_z = \{\mu\sigma^{\frac{1}{2}}P/(\rho\nu)^{\frac{1}{2}}(D^2-4)\}[D(a^2-r^2)/2 + \frac{a^2\cosh\{D\ln(r/a\delta)\} + a^2\delta - {}^2a^2\delta\cosh\{D\ln(r/a)\} - a^2\cosh M^*]}{\sinh M^*}. \tag{105}$$

M^*, ϕ, etc., are defined by the equations (65), with $\theta_0 = 2\pi$. The solutions are well behaved at $D = 2$. Globe (1959) has plotted some of the characteristics of the flow for moderate values of M^*. As usual, it is instructive to examine the flow in the limit of large Hartmann number. It follows from the equations (65) that

$$k_a = \bar{k} = \text{constant}. \tag{106}$$

It can now be deduced from equation (103) that V_z is of order $(Pa^2/\rho\nu\,(M^*)^{-2}$, in the core. This result can be confirmed by taking the limit of equation (104). The latter equation also shows that V_z is everywhere positive. Equation (101) gives the value of $B_z(a)$ as $\{\mu a^2(1-\delta^2)\,P\sigma^{\frac{1}{2}}/2(\rho\nu)^{\frac{1}{2}}\,D\}$. This result can be confirmed by taking the limit of (105) as $M^* \to \infty$. Equation (103) gives $(j_\phi)_c = 0$. In fact, $j_\phi = j_r = 0$ for all M^*. The boundary layers on the walls are not full Hartmann layers. That is to say, there is no concentration of current in them.

(ii) *Other special cases*

The radial field has the property $B_0 = B_0(\phi)$. This is also true of a uniform field. No other applied magnetic field has this property. Thus in all other cases, the features noted in the first part of this section will apply. Heiser & Shercliff (1965) carried out an experiment using a magnet which provides a radial field. However, their flow was an azimuthal one ($\mathbf{V} = V\hat{\boldsymbol{\theta}}$). This was a vital feature of the experiment because the yoke of the magnet closed off the annular gap, at one of the ends. In Hartmann flows an axial motion occurs. It seems likely therefore that a duct in the form of a double annulus would be required. These would be joined up near the closed end of the magnet. If this is not done, one is faced with the problem of passing the fluid through the yoke of the magnet. The above comments apply for all 'radial-type' fields.

8. Remarks

The main feature of the foregoing discussion is the choice of co-ordinate systems. The equations under review are of the type

$$\left.\begin{aligned} \nabla^2 v + (\mathbf{B}_0.\nabla)\,b &= f_1(x,y), \\ \text{and} \qquad \nabla^2 b + (\mathbf{B}_0.\nabla)\,v &= f_2(x,y), \end{aligned}\right\} \tag{107}$$

where b and v are functions of x and y only. Furthermore, $\mathbf{B}_0$ is a vector whose divergence and curl are zero. $\mathbf{B}_0$ lies in the (x, y)-plane and its components depend only on those two variables. It has been shown that the system of equations,

(107), can be greatly simplified by working in the co-ordinate system traced out by the vector $\mathbf{B}_0$.

The paper has concentrated largely on the high Hartmann number situation. This is because, in this limit, many interesting features can be extracted without much further restriction on $\mathbf{B}_0$. Also, the walls of the pipe were taken to be insulators. Even so, all the many possibilities have not been exhausted. Much more can be done on insulating ducts as well as on ducts with conducting walls. It is contended that many novel features have been revealed in this paper and it is hoped that the work will inspire some experiments. (A suitably curved, non-uniform, cylindrical field exists near the edges of the plane pole faces on those magnets which are used to create uniform fields.) The specific examples taken in this paper were circular and radial fields. The analysis for other fields is relatively cumbersome though technically straightforward. It is to be hoped that further work on other applied magnetic field distributions will be carried out. In particular, cases where neutral points occur within the duct deserve attention.

Lastly, the type of analysis employed in this paper deserves comment. The assumption of insulating walls reduces the problem to the solution of a second order, linear, elliptic, partial differential equation of the form

$$\nabla^2 m + M^* \frac{\partial m}{\partial x} = h(x, y),$$

where M^* is a constant and h is known, and properties of the solution have been obtained by singular perturbation analysis in the limit of large M^*. A general analysis of problems of this type has been given by Eckhaus & de Jager (1966). They treat an equation of the form

$$\{L_2(x, y)\} m + M^* \left\{ \frac{\partial}{\partial y} + g(x, y) \right\} m = h(x, y), \tag{108}$$

where L_2 is a linear, elliptic partial differential operator of the second order and h is known, and they carry out singular perturbation analyses in the limit of large M^*. They deal with simply connected regions and Dirichlet boundary conditions. Thus their work is directly relevant to that of §§3–5. They find that discontinuities ('wakes'), if they arise, occur along the lines x = constant, and that these are diffused by the elliptic term. This is the generalization of what is found in §3(ii). Eckhaus & de Jager also analyse 'side' boundary layers of the type which arose in §4. They give an integral expression whose appropriate series expansion is the generalization of the series given in §4. Finally they give a rigorous account of the magnitude of neglected terms, small singular regions, etc. This provides valuable background to the present paper.

REFERENCES

Eckhaus, W. & de Jager, E. M. 1966 *Arch. Rat. Mech. Anal.* **23**, 26.

Globe, S. 1959 *Phys. of Fluids*, **2**, 404.

Heiser, W. H. & Shercliff, J. A. 1965 *J. Fluid Mech.* **22**, 701.

Morse, P. M. & Feshbach, H. 1953 *Methods of Theoretical Physics*, Volume 1. London: McGraw Hill.

Shercliff, J. A. 1953 *Proc. Camb. Phil. Soc.* **49**, 136.

Shercliff, J. A. 1965 *A Textbook of Magnetohydrodynamics*. Oxford: Pergamon Press.

Todd, L. 1967 *J. Fluid Mech.* **28**, 371.